

Chiroptical Properties, Electronic Structure, and Multicenter Bonding in a Dissymmetric Binuclear Beryllium Alkyl Complex: $\text{Be}_2(\text{C}(\text{CH}_3)_2)_2$

D. K. Jha¹¹Lunglei Government College, Lunglei, Mizoram, India. PIN 796701

Publication Date: 2026/04/09

Abstract The electronic structure, bonding, and chiroptical signatures of the binuclear beryllium complex $\text{Be}_2(\text{C}(\text{CH}_3)_2)_2$ were characterized using density functional theory (DFT) and topological analysis. The results reveal a remarkably short Be–Be distance of 1.9219 Å with a Mayer bond order (MBO) of 0.705. Topological analysis via the Electron Localization Function (ELF) and Atoms in Molecules (AIM) identifies a framework stabilized by multicentre Be–C–Be interactions rather than a direct metal–metal covalent bond. The simulated UV–Vis and Electronic Circular Dichroism (ECD) spectra exhibit a prominent feature at 362.3 nm, identified through Natural Transition Orbital (NTO) analysis as a metal-centered σ to σ^* excitation with significant charge-transfer character.

Keywords: LOL, ELF, ECD, NTO, AIM, Be-Be Bonds, Organoberyllium, DFT, EDA-NOCV, Chiroptical Property, Cotton Effect.

How to Cite: D. K. Jha (2026) Chiroptical Properties, Electronic Structure, and Multicenter Bonding in a Dissymmetric Binuclear Beryllium Alkyl Complex: $\text{Be}_2(\text{C}(\text{CH}_3)_2)_2$. *International Journal of Innovative Science and Research Technology*, 11(4), 56-60. <https://doi.org/10.38124/ijisrt/26apr180>

I. INTRODUCTION

The exploration of group 2 metal–metal bonding remains a significant frontier in modern organometallic research. Traditionally, alkaline earth metals are characterized by a closed-shell ns^2 electronic configuration, which typically favours the formation of ionic species or classical two-centre-two-electron bonds in higher oxidation states. Within this group, binuclear beryllium species are exceptionally rare and historically elusive.¹⁻¹⁴ The stabilization of such species generally necessitates the use of specialized ligand frameworks to overcome the inherent electronic repulsion of the metal centres.

Among recent computational targets, the complex $\text{Be}_2(\text{C}(\text{CH}_3)_2)_2$ stands out for its compact binuclear core and its unique potential for axial chirality. Previous studies in the field have relied heavily on standard geometry optimizations, yet the nuanced nature of metal–ligand interactions in these low-valent systems requires more sophisticated analytical approaches. By employing advanced topological and spectroscopic tools, including Atoms in Molecules (AIM) and Electron Localization Function (ELF) mapping, we seek to elucidate the fundamental nature of the Be–Be interaction and determine whether it constitutes a direct covalent bond or a multicentre network.^{15,16}

Furthermore, the dissymmetric nature of this alkyl complex provides an opportunity to investigate the origin of its chiroptical response. This study utilizes Time-Dependent

Density Functional Theory (TD-DFT) and Natural Transition Orbital (NTO) analysis to resolve the singlet excited states and define the diagnostic chiroptical fingerprints that characterize the absolute configuration of the binuclear cluster. Through this synergy of topological bonding analysis and simulated spectroscopy, we provide a comprehensive framework for understanding the electronic structure of dissymmetric group 2 organometallics.

II. COMPUTATIONAL METHODS

Ground-state geometry optimization and vibrational frequency analyses were performed using the ORCA 6.1.1 program package at the TPSS/def2-TZVP level of theory.¹⁷⁻¹⁸ Resolution of identity (RI) approximations with the def2/J auxiliary basis were utilized. Time-dependent DFT (TD-DFT) was employed to resolve the first 15 singlet excited states and simulate the ECD and UV–Vis spectra.¹⁹ Natural Bond Orbital (NBO) analysis and second-order perturbation theory (SOPT) were conducted to evaluate hyperconjugative stabilization.²⁰ Topological characterization, including AIM, Laplacian, LOL, ELF mapping, and fuzzy atomic space analysis, was performed using Multiwfn 3.8.²¹

III. RESULTS AND DISCUSSION

➤ Molecular Structure and Thermochemistry

The optimized geometry of $\text{Be}_2(\text{C}(\text{CH}_3)_2)_2$ exhibits a bridged binuclear structure with a Be–Be bond length of 1.9219 Å. The Be–C bond lengths average 1.732 Å,

consistent with typical organoberyllium species. Frequency calculations confirmed the structure as a true minimum on the potential energy surface. The total entropy term (TS) at 298.15 K was determined to be 29.10 kcal/mol, primarily driven by translational (11.86 kcal/mol) and rotational (8.53 kcal/mol) components.

➤ Bonding and Topological Analysis

The nature of the Be–Be interaction was scrutinized through multiple bonding indices. Mayer Bond Order (MBO) analysis yields a value of 0.705, suggesting a robust interaction despite the absence of a formal NBO bond. SOPT identifies significant stabilization (9.0 kcal/mol) through hyperconjugation between the C–Be bonding orbitals and methyl C–H antibonding orbitals.

Table 1 Summary of Bonding Indices and Topological Properties

Interaction Type	MBO ^a	FBO ^b	MCI (3-Center) ^c	ELF Basin Type	Local. (Hole/Elect. %) ^d
Be–Be (direct)	0.705	0.184	—	Depleted core	46.0 / 26.0
Be–C (bridge)	0.89	0.429	—	Shared-electron	33.2 / 50.9
Be–C–Be (bridge)	—	—	0.169	Multicenter basin	—

• Table Footnotes and Methods:

✓ ^a MBO:

Mayer Bond Order calculated at the TPSS/def2-TZVP level in ORCA.

✓ ^b FBO:

Fuzzy Bond Order derived from the Atomic Overlap Matrix (AOM) in Multiwfn using Becke partitioning.

✓ ^c MCI:

Multi-Center Index for the 3-center Be–C–Be interaction, indicating strong cooperative bonding.

✓ ^d Localization:

Percentage of the Natural Transition Orbital (NTO) hole (27a) and electron (28a) localized on the respective atomic basins.

✓ ELF Basin Type:

Qualitative classification based on the Electron Localization Function map.

AIM topological analysis confirms the multicenter character of the core. While no (3,-1) bond critical point (BCP) is found directly between the Beryllium atoms, two (3,+1) ring critical points (RCPs) are identified within the Be–C–Be triangular motifs. This is complemented by the ELF map, which shows high localization basins between Be and bridging C atoms but depletion along the Be–Be axis. Fuzzy atomic overlap matrix (AOM) analysis provides a Multi-Centre Index (MCI) of 0.169 for the Be–C–Be bridge, formally classifying the system as a 3-center-2-electron (3c-2e) bonded cluster.

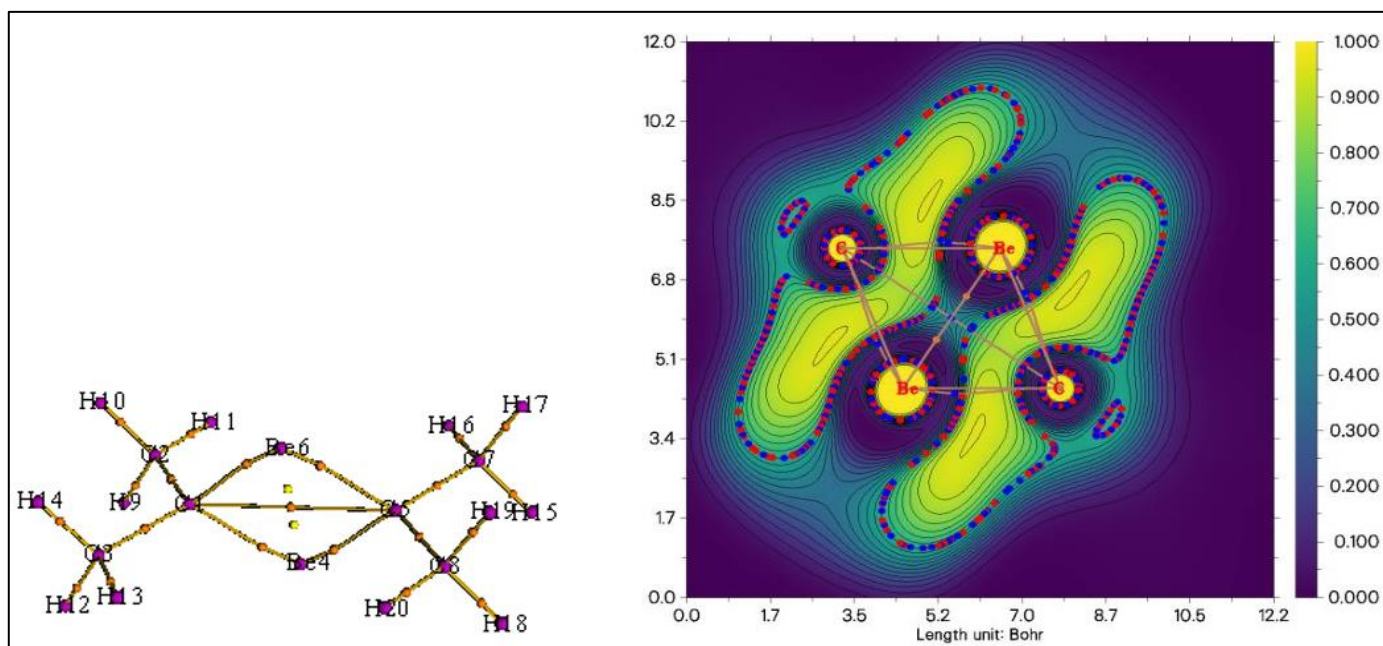


Fig 1 AIM Topology and ELF Map

➤ Excited States and NTO Analysis

The UV–Vis absorption spectrum is dominated by the S₃ state at 362.3 nm with a high oscillator strength of $f =$

0.2766\$. Natural Transition Orbital (NTO) analysis reveals that this transition is 96.87% characterized by the 27a to 28a pair.

- *Orbital 27a (Hole):*
Concentrated as a σ -bonding lobe between the Be atoms, localized 46% on the metallic core.
- *Orbital 28a (Electron):*
Exhibits an antibonding node between Be atoms with 51% localization on the carbon ligands, signifying a σ to σ^*

transition with metal-to-ligand charge transfer (MLCT) character.

Higher-energy transitions (States 8 and 9) involve delocalization from the framework-stabilizing orbital (26a) to diffuse orbitals (29a) extending over the methyl hydrogens.

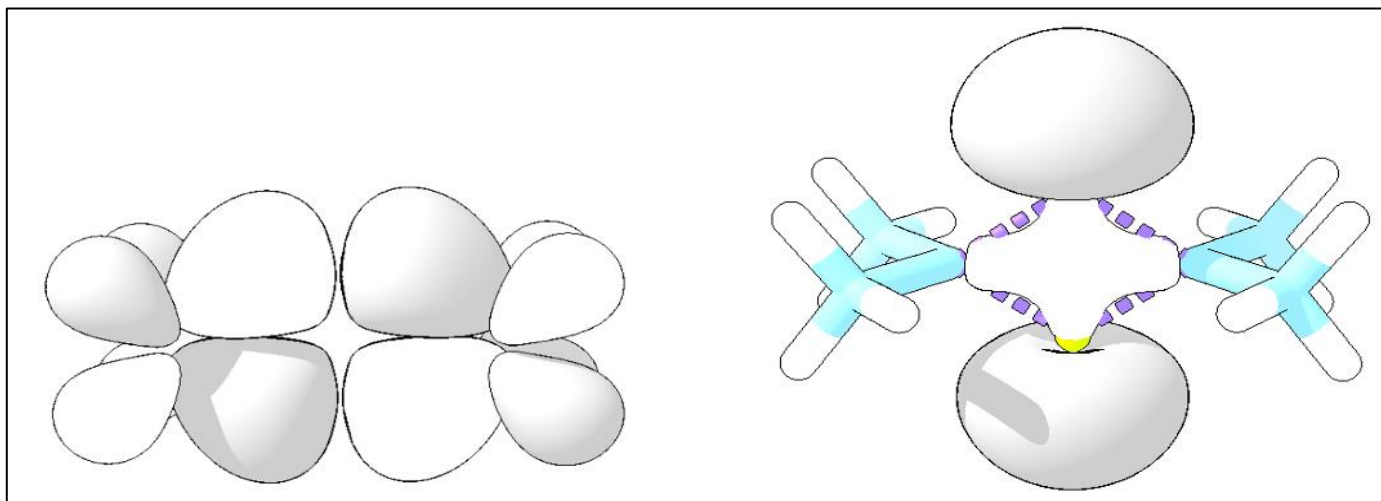


Fig 2 NTO Hole (27a) and Electron (28a) Pairs

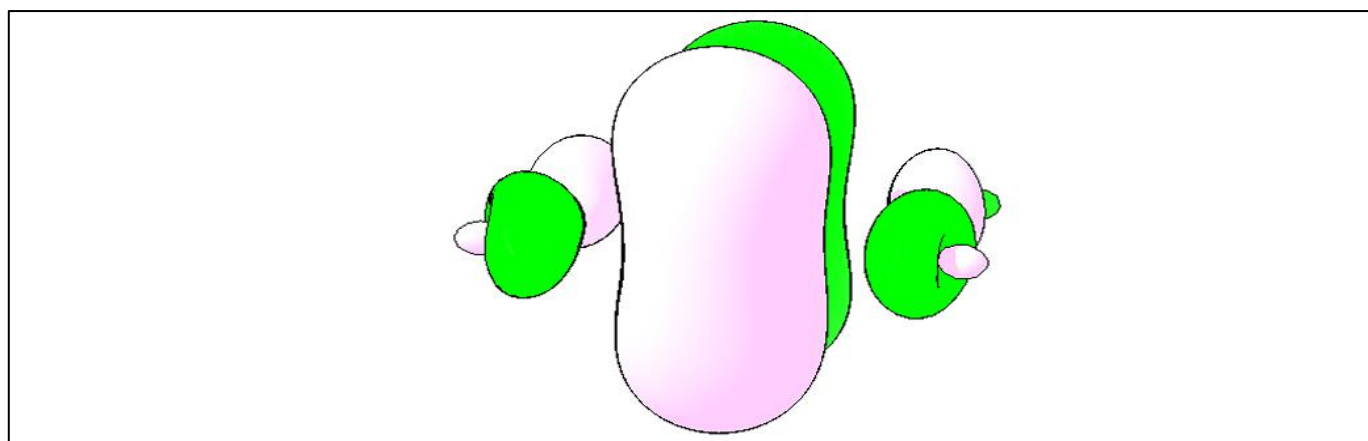


Fig 3 NTO electron 29a

➤ Chiroptical Properties

The ECD spectrum displays a significant negative Cotton effect at 362 nm, coinciding with the UV-Vis maximum. This rotatory strength arises from the

dissymmetric twist of the methyl-substituted carbon bridge, making the 362 nm signal a unique chiroptical fingerprint for the (R) or (S) absolute configuration of the binuclear cluster.

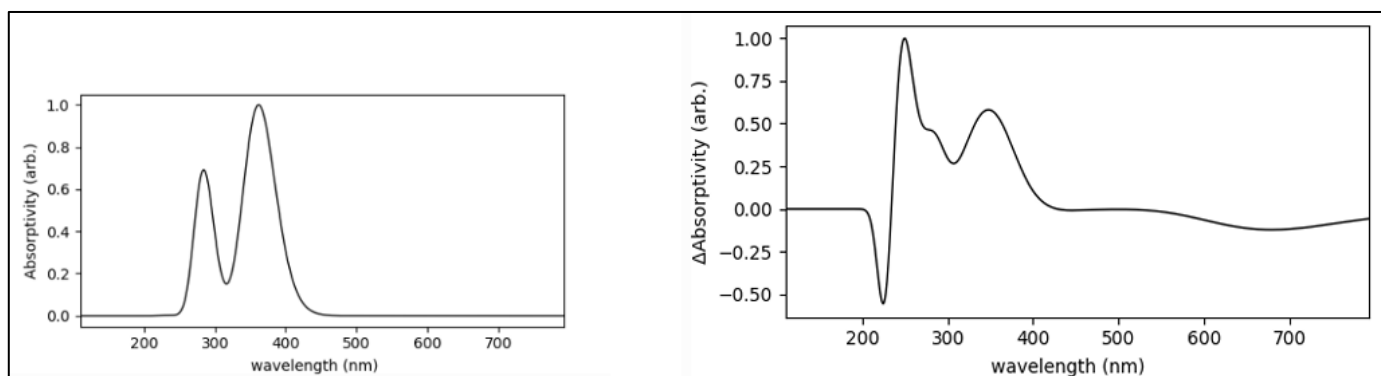


Fig 4 Simulated UV-Vis and ECD Spectra

➤ EDA-NOCV

Energy Decomposition Analysis (EDA) and the Extended Transition State-Natural Orbitals for Chemical Valence (ETS-NOCV) results, represent the charge deformation densities ($\Delta\rho_k$) corresponding to specific bonding channels in the molecule. In these plots, the purple and gold isosurfaces represent areas of charge accumulation and depletion during bond formation.

NOCV Deformation Densities

• NOCV Pair 0 (Primary Bonding):

This channel is the most significant contributor to the orbital stabilization energy ($\Delta E_1 = -55.24$ kcal/mol) with the highest eigenvalue of 0.7766. The plot shows a high degree of charge accumulation between the two beryllium centers, confirming the strong σ -type interaction described in the NTO analysis.

• NOCV Pair 1 (Multicenter Bridging):

With an eigenvalue of 0.3098 and an energy contribution of -18.56 kcal/mol, this channel represents the

stabilization arising from the multicenter Be–C–Be framework. The deformation density shows charge redistribution extending from the bridging carbon atoms toward the beryllium core, diagnostic of the 3-center-2-electron (3c-2e) bonding identified via topological indices (MCI = 0.169).

• NOCV Pair 2 (Ligand-Metal Delocalization):

This pair ($\Delta E_3 = -7.26$ kcal/mol) represents secondary delocalization and back-donation effects. The isosurfaces illustrate charge flow from the alkyl ligand framework into the vacant orbitals of the beryllium core.

• NOCV Pairs 3 & 4 (Hyperconjugation and Symmetry Adjustments):

These lower-energy channels (-6.0 to -2.5 kcal/mol) correspond to the hyperconjugative stabilization between C–Be bonding orbitals and methyl C–H antibonding orbitals noted in the second-order perturbation theory (SOPT) analysis.

Table 2 Summary of Bonding Contributions

Plot/Channel	Eigenvalue (e)	ΔE_{orb} (kcal/mol)	Bonding Character
NOCV 0	0.7766	-55.24	Core σ -bonding
NOCV 1	0.3098	-18.56	3c-2e Be–C–Be bridge
NOCV 2	0.1619	-7.26	Framework delocalization
NOCV 3	0.1016	-6.08	Hyperconjugative stabilization
NOCV 4	0.0909	-2.51	Ligand-based delocalization

The overall bonding is governed by a synergetic effect where large electrostatic attractions ($\Delta E_{elstat} = -206.76$ kcal/mol) are complemented by these specific orbital deformation channels, resulting in a total bond energy of -104.81 kcal/mol relative to the triplet fragments.

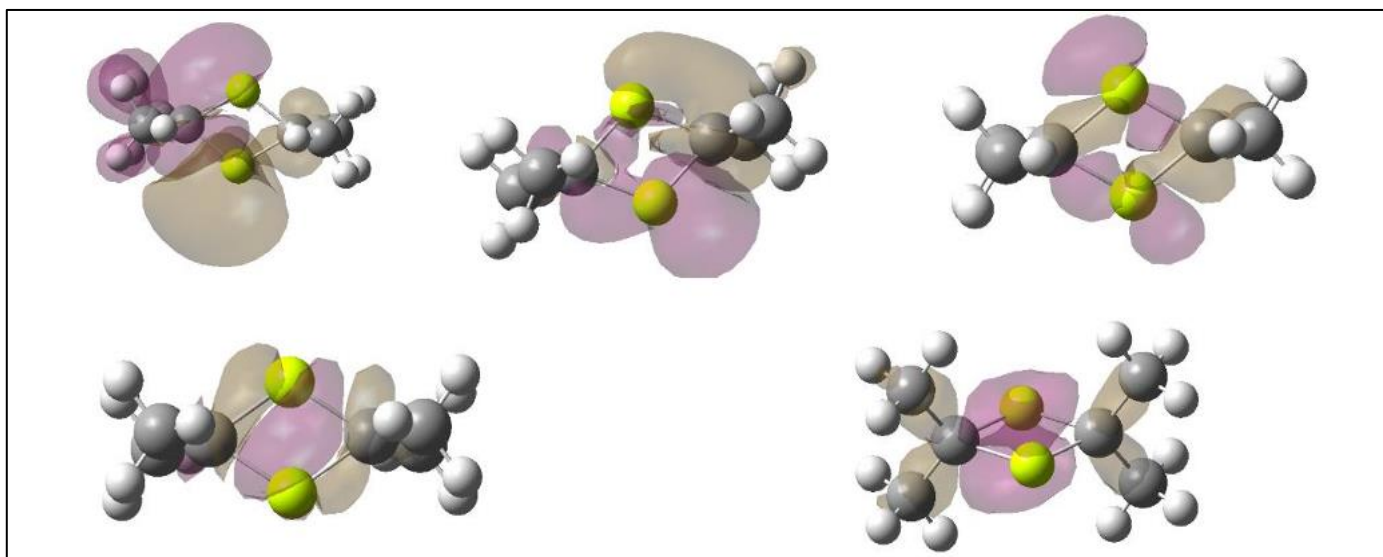


Fig 5 NOCV Deformation Densities of NOCV0, NOCV1, NOCV2, NOCV3, NOCV4

IV. CONCLUSION

This study provides a comprehensive description of the electronic and structural properties of $\text{Be}_2(\text{C}(\text{CH}_3)_2)_2$. The short Be–Be interaction (1.92 Å) is maintained by multicentre 3c-2e bridging rather than a direct covalent bond.

The electronic excitation at 362 nm is defined by a metal-centered σ to σ^* transition that serves as a diagnostic spectroscopic marker. The synergy between topological bonding analysis and chiroptical signatures offers a robust framework for characterizing low-valent group 2 organometallics.

REFERENCES

- [1]. DK Jha, Beryllium-Trapped Electride Electrons: A Stable Non Nuclear Bridge in Triazole Dimers. *IJCRD* 2026; 8(3): 14-18. DOI: 10.33545/26646552.2026.v8.i3a.123
- [2]. DK Jha, σ -Aromatic Stabilization of a Be₄ Core by NH Ligands: DFT Study, *IJCRD* 2026; 8(3): 06-13. DOI: 10.33545/26646552.2026.v8.i3a.122
- [3]. Z. H. Cui, W. S. Yang, L. Zhao, Y. H. Ding, G. Frenking (2016). *Angew. Chem. Int. Ed.*, 55, 7841; *Angew. Chem.* 2016, 128, 7972.
- [4]. Ariyaratna, I. R. and E. Miliordos (2020). "Be-Be Bond in Action: Lessons from the Beryllium-Ammonia Complexes [Be(NH(3))(0-4)](2)(0,2)." *J Phys Chem A* 124(47): 9783-9792.
- [5]. Cong, F., et al. (2023). "Beryllium Dimer Reactions with Acetonitrile: Formation of Strong Be-Be Bonds." *Molecules* 29(1)
- [6]. Dong, X., et al. (2023). "B(7) Be(6) B(7) : A Boron-Beryllium Sandwich Complex." *Angew Chem Int Ed Engl* 62(31): e202304997. DOI/10.1002/anie.202304997
- [7]. Goesten, M. G. (2022). "Be-Be pi-Bonding and Predicted Superconductivity in MBe(2) (M=Zr, Hf)." *Angew Chem Int Ed Engl* 61(4): e202114303
- [8]. Michael C. Heaven, Vladimir E. Bondybey, Jeremy M. Merritt, Alexey L. Kaledin. (2011). "The unique bonding characteristics of beryllium and the Group IIA metals." *Chemical Physics Letters* 506(1-3): 1-14
- [9]. Michael C. Heaven, Jeremy M. Merritt, and Vladimir E. Bondybey. (2011). "Bonding in beryllium clusters." *Annu Rev Phys Chem* 62: 375-393.
- [10]. Mazumder, L. J. and A. K. Guha (2023). "Three-membered beryllium ring, Be(3): not just a hydrogen bond acceptor." *Phys Chem Chem Phys* 25(31): 20947-20950
- [11]. Jeremy M Merritt, Vladimir E Bondybey, Michael C Heaven. (2009). "Beryllium dimer--caught in the act of bonding." *Science* 324(5934): 1548-1551.
- [12]. Shahnaz S Rohman, Chayanika Kashyap, Sabnam S Ullah, Ankur K Guha, Lakhya J Mazumder, Pankaz K Sharma. (2019). "Ultra-Weak Metal-Metal Bonding: Is There a Beryllium-Beryllium Triple Bond?" *Chem. Phys. Chem.* 20(4): 516-518
- [13]. Wen-Yan Tong, Tao-Tao Zhao, Xue-Feng Zhao, Xiaotai Wang, Yan-Bo Wu, Caixia Yuan. (2019). "Neutral nano-polygons with ultrashort Be-Be distances". *Dalton Trans* 48(42): 15802-15809.
- [14]. Eva Vos, Inés Corral, M. Merced Montero-Campillo, Otilia M^o, José Elguero, Ibon Alkorta and Manuel Yáñez. (2021). "Spontaneous bond dissociation cascades induced by Be(n) clusters (n = 2,4)". *Phys Chem Chem Phys* 23(11): 6448-6454
- [15]. Bader, R. F. W. *Atoms in Molecules: A Quantum Theory*, Oxford University Press, 1990.
- [16]. T.Lu, Visualization Analysis of Covalent and Noncovalent Interactions in Real Space. *Angew. Chem. Int. Ed.* 2025, 64, e202504895. <https://doi.org/10.1002/anie.202504895>
- [17]. Neese, F. Software update: the ORCA program system, version 6.0, *WIREs Comput. Molec. Sci.* 2025, 15, e70019.
- [18]. Neese, F. Software update: The ORCA program system, version 5.0, *WIREs Comput. Molec. Sci.* 2022, 12, e1606.
- [19]. Cárdenas Sabando, R.; Riplinger, C.; Wennmohs, F.; Neese, F.; Bistoni, G. Broadening the Scope of the ETS-NOCV scheme: A Versatile Implementation in ORCA, *J. Chem. Theory Comput.* 2025, doi.org/10.1021/acs.jctc.5c01003.
- [20]. Weinhold, F.; Landis, C. R. *Discovering Chemistry With Natural Bond Orbitals*, Wiley, 2012.
- [21]. Lu, T.; Chen, F. Multiwfn: A multifunctional wavefunction analyzer, *J. Comput. Chem.* 2012, 33, 580-592.